

Supporting Information

Investigation on the Interaction Mechanism of Different SARS-CoV-2 Spike Variants with hACE2: Insights from Molecular Dynamics Simulations

Jianhua Wu,[†] Hong-Xing Zhang^{†,*} and Jilong Zhang,^{†,*}

[†]Institute of Theoretical Chemistry, College of Chemistry, Jilin University, Changchun 130023, Jilin, People's Republic of China.

*Emails: jilongzhang@jlu.edu.cn; zhanghx@jlu.edu.cn

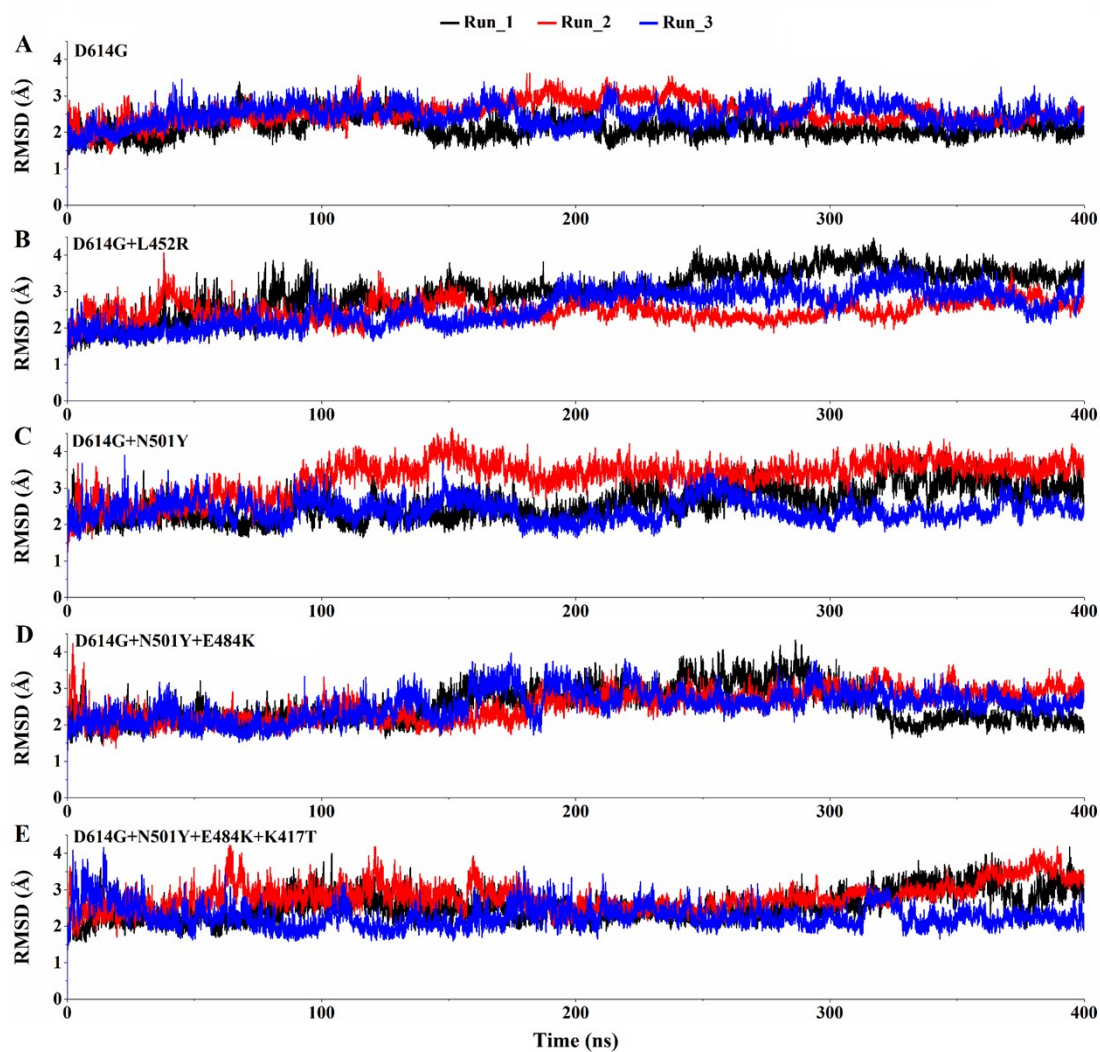


Fig S1. The time evolution of the root mean square deviation (RMSD) during the Run_1 (black), Run_2 (red), and Run_3 (blue) for 400 ns simulations of (A) D614G, (B) D614G+L452R, (C) D614G+N501Y, (D) D614G+N501Y+E484K, and (E) D614G+N501Y+E484K+K417T mutants, respectively.

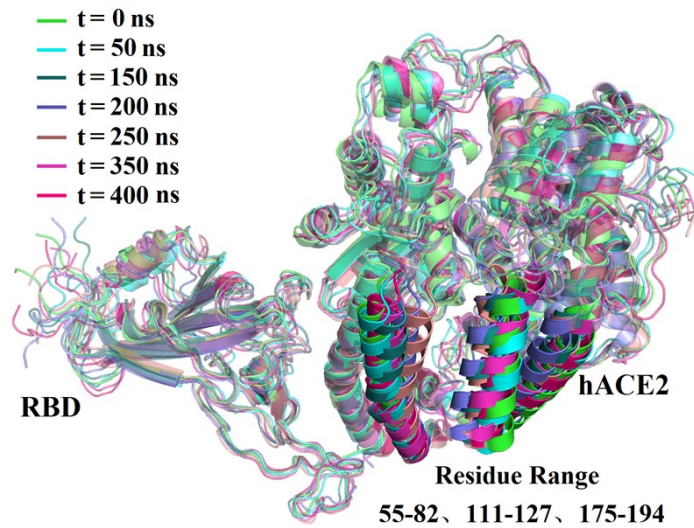


Fig S2. Superimposed 3D structures of the D614G+N501Y+E484K mutant with its initial structure ($t = 0$ ns) at different MD simulation periods ($t = 50, 150, 200, 250, 350,$ and 400 ns). Regions with large RMSD fluctuations are represented as solids, while other regions are represented as transparent.

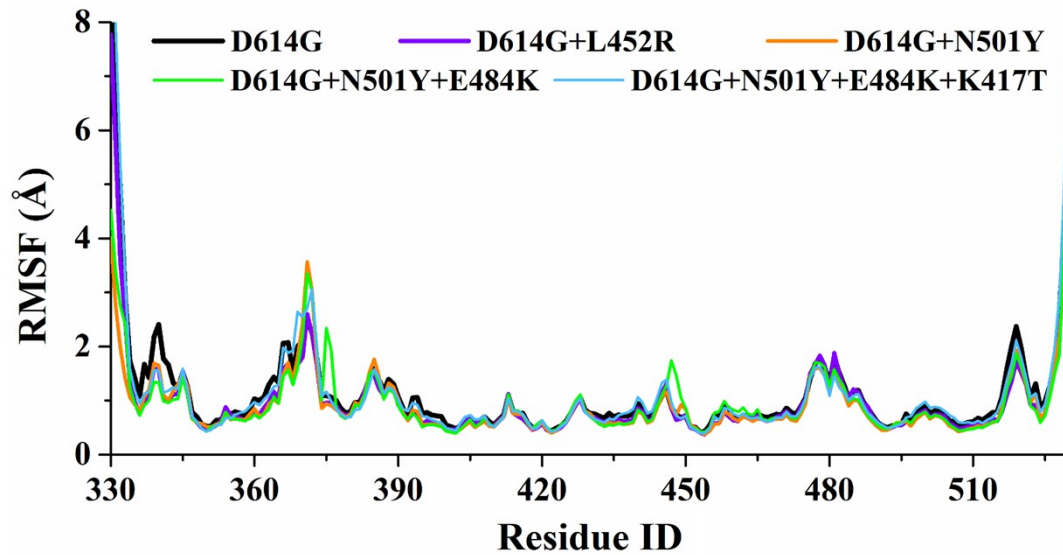


Fig S3. RMSF plots of replica simulations for five systems D614G (black), D614G+L452R (violet), D614G+N501Y (orange), D614G+N501Y+E484K (green), and D614G+N501Y+E484K+K417T (blue) variants, respectively.

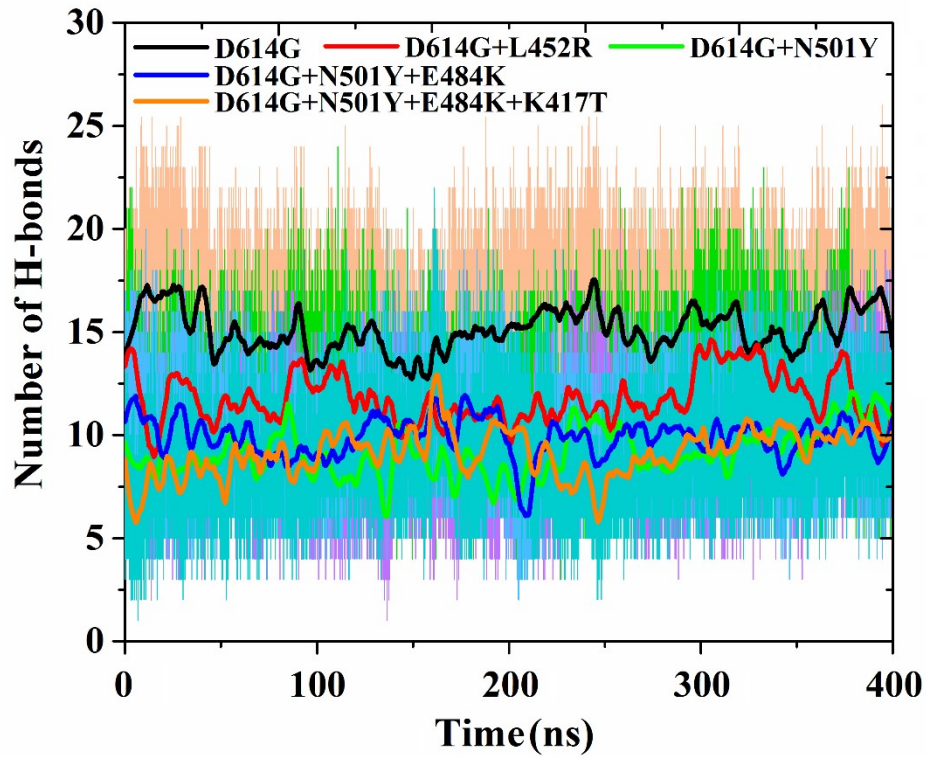


Fig S4. A comparison of the number of H-bonds of replica simulations between the hACE2 and RBD of D614G (black) singly mutated, D614G+L452R (red) and D614G+N501Y (green) doubly mutated, D614G+N501Y+E484K (blue) triply mutated, and D614G+N501Y+E484K+K417T (orange) quadruply mutated variant RBDs during the MD simulations.

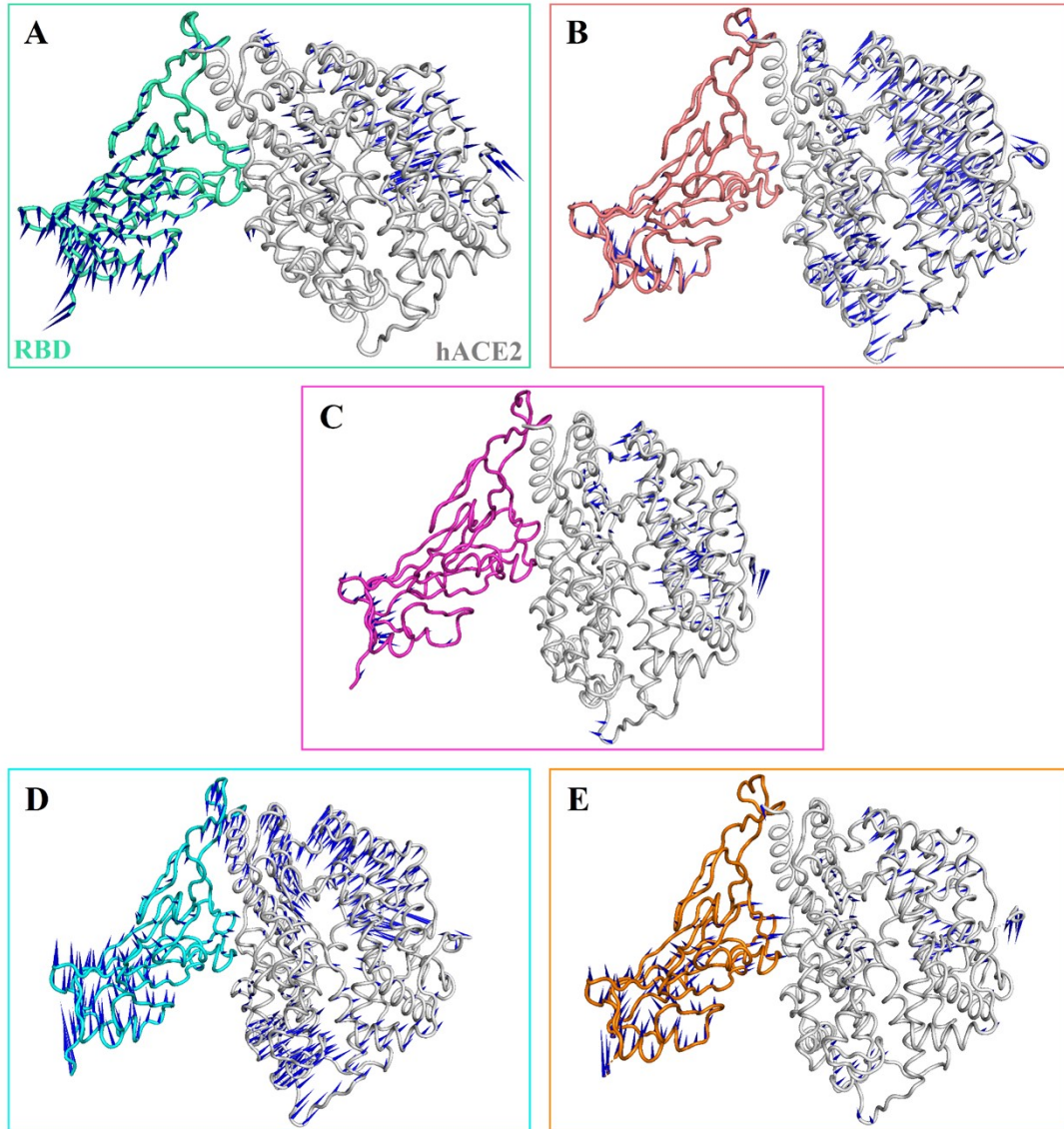


Fig S5. Representation of the dominant motions of the RBD and hACE2 residues obtained from the first principal component (PC1) in the replica simulations for the complexes established with (A) D614G (green cyan), (B) D614G+L452R (salmon), (C) D614G+N501Y (light magenta), (D) D614G+N501Y+E484K (cyan), (E) D614G+N501Y+E484K+K417T (orange).

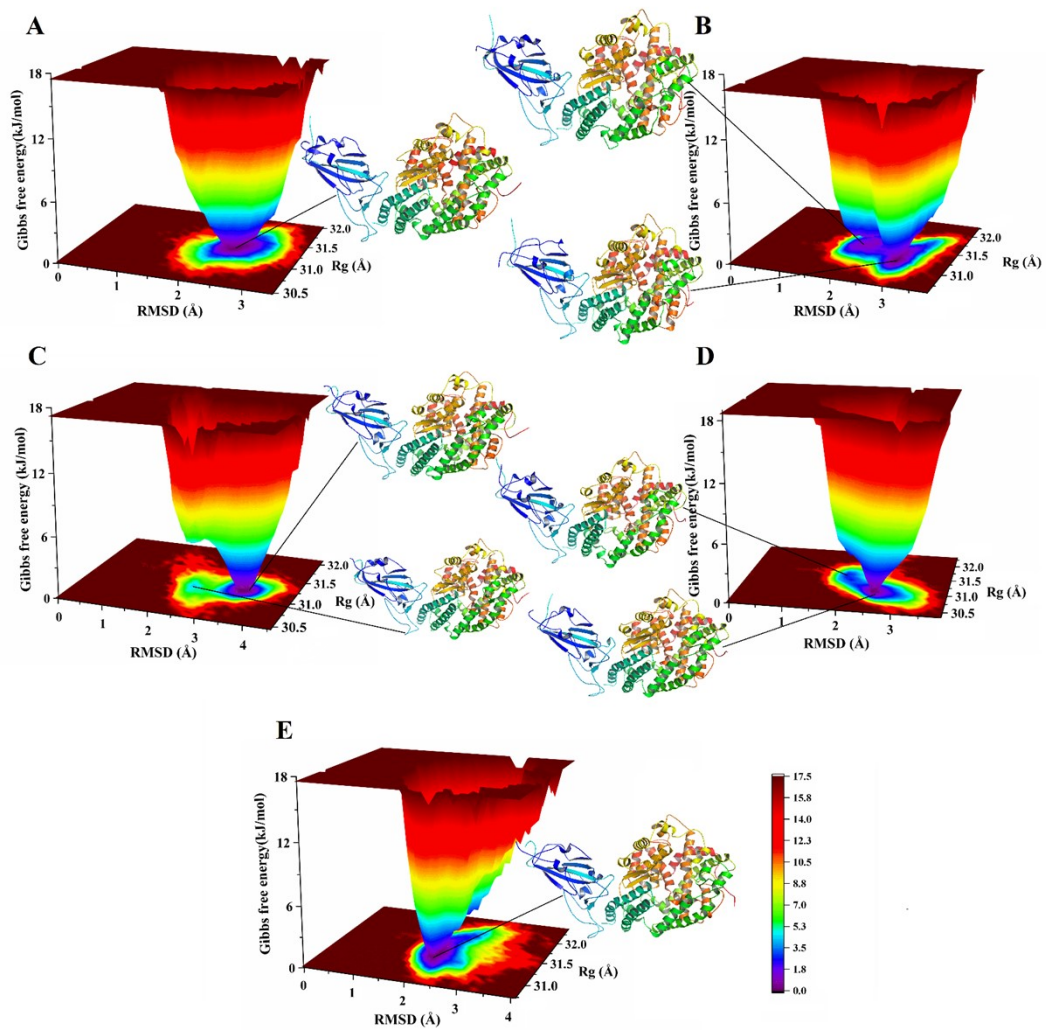


Fig S6. Free energy landscapes of (A) D614G, (B) D614G+L452R, (C) D614G+N501Y, (D) D614G+N501Y+E484K, and (E) D614G+N501Y+E484K+K417T complexes during the replica MD simulations. The graphs were projected on the RMSD and Rg values for C α atoms.

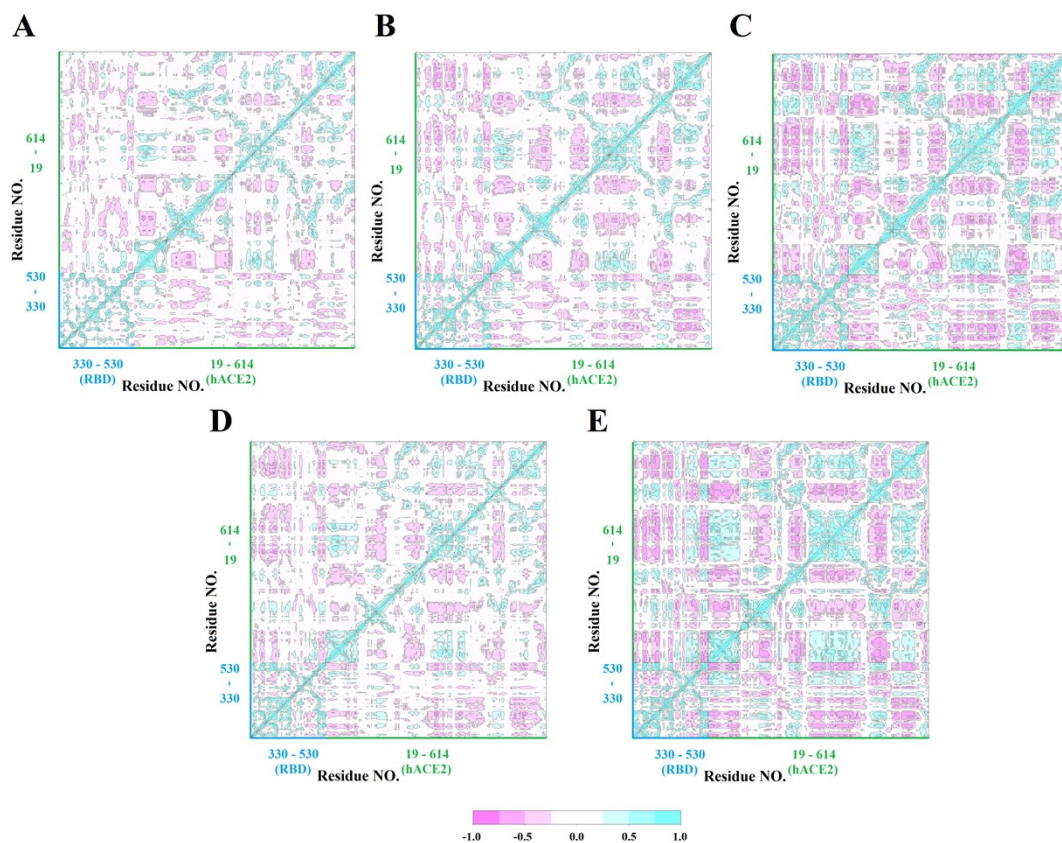


Fig S7. Dynamic cross-correlation map of the $C\alpha$ atoms of the (A) D614G, (B) D614G+L452R, (C) D614G+N501Y, (D) D614G+N501Y+E484K, and (E) D614G+N501Y+E484K+K417T complexes in the replica simulations. X-axis: RBD residue IDs from 330 to 530 are shown in light blue, hACE2 residue IDs from 19 to 614 are shown in green.

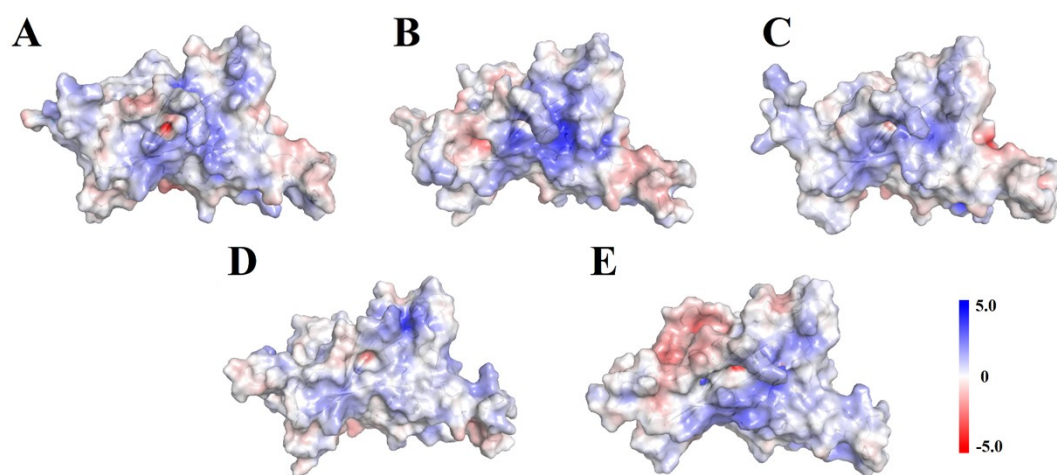


Fig S8. Electrostatic potential map of RBDs for (A) D614G, (B) D614G+L452R, (C) D614G+N501Y, (D) D614G+N501Y+E484K, and (E) D614G+N501Y+E484K+K417T in the replica simulations.

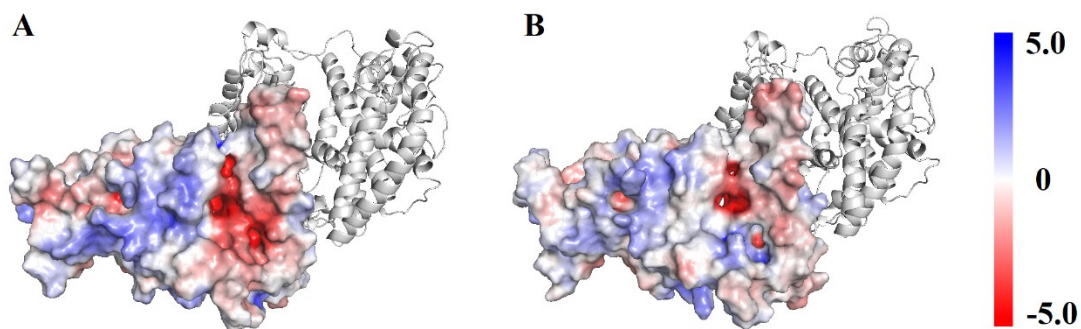


Fig S9. Electrostatic potential map of the interaction interface of RBD and hACE2 for (A) D614G+L452R and (B) D614G+N501Y+E484K.

Table S1. The computed binding energy of hACE2 with all RBD variants using MM/PBSA method in the replica simulations. All energies are in kcal/mol.

System	D614G		D614G+L452R		D614G+N501Y		D614G+N501Y+E484K		D614G+N501Y+E484K+K417T	
	Run_2	Run_3	Run_2	Run_3	Run_2	Run_3	Run_2	Run_3	Run_2	Run_3
van der Waals energy	-89.2±0.2	-89.6±0.2	-91.0±0.2	-85.0 ±0.2	-86.7 ±0.2	-90.3 ±0.2	-88.0 ±0.2	-90.0 ±0.2	-88.2 ±0.2	-89.3 ±0.2
Electrostatic energy	-388.7±0.7	-392.6±0.7	-458.9 ±0.7	-446.8 ±0.7	-362.8 ±0.7	-354.3 ±0.6	-505.5 ±0.7	-501.2 ±0.7	-391.9 ±0.6	-408.4 ±0.6
Polar solvation energy	224.8±1.4	250.0±1.1	242.7 ±1.2	239.6 ±1.4	177.4 ±1.4	178.7 ±1.1	139.6 ±1.3	165.7 ±1.2	135.8 ±1.0	148.8 ±1.2
SASA energy	-10.9±0.0	-10.8±0.0	-10.9 ±0.0	-10.5 ±0.0	-10.1 ±0.0	-10.4 ±0.0	-10.3 ±0.0	-10.6 ±0.0	-10.3 ±0.0	-10.3 ±0.0
Binding free energy	-263.8±1.2	-242.9±1.1	-318.1±1.1	-302.8±1.2	-282.2±1.3	-276.3±1.1	-464.2±1.0	-436.1±1.1	-354.6±1.0	-359.2±1.1

Table S2. Individual contributions of mutation site residues on the D614G and its variant RBDs to the energy component of residue-based energy decomposition. Energy values are given in units of kcal/mol.

System	Residue	MM energy	Polar energy	Non-polar energy	Total energy
D614G	Lys417	-61.80	21.88	-0.17	-40.09
	Leu452	-0.44	0.16	0.00	-0.28
	Glu484	39.58	4.68	-0.05	44.22
	Asn501	-8.03	8.74	-0.20	0.52
D614G+L452R	Arg452	-38.10	0.88	0.00	-37.22
D614G+N501Y	Tyr501	-8.31	6.25	-0.45	-2.50
D614G+N501Y+E484K	Lys484	-43.97	-1.25	-0.02	-45.24
	Tyr501	-6.37	4.57	-0.39	-2.19
D614G+N501Y+E484K+K417T	Thr417	-0.91	0.30	-0.01	-0.62
	Lys484	-39.67	-2.09	-0.02	-41.77
	Tyr501	-7.17	5.34	-0.38	-2.22